Electronic Supplementary Material (ESI)

Environmental reactions of air-quality protection on eco-friendly iron-based catalysts

Melissa Greta Galloni‡[1], Sebastiano Campisi‡[1], Sergio Gustavo Marchetti[2], Antonella Gervasini[1,*]

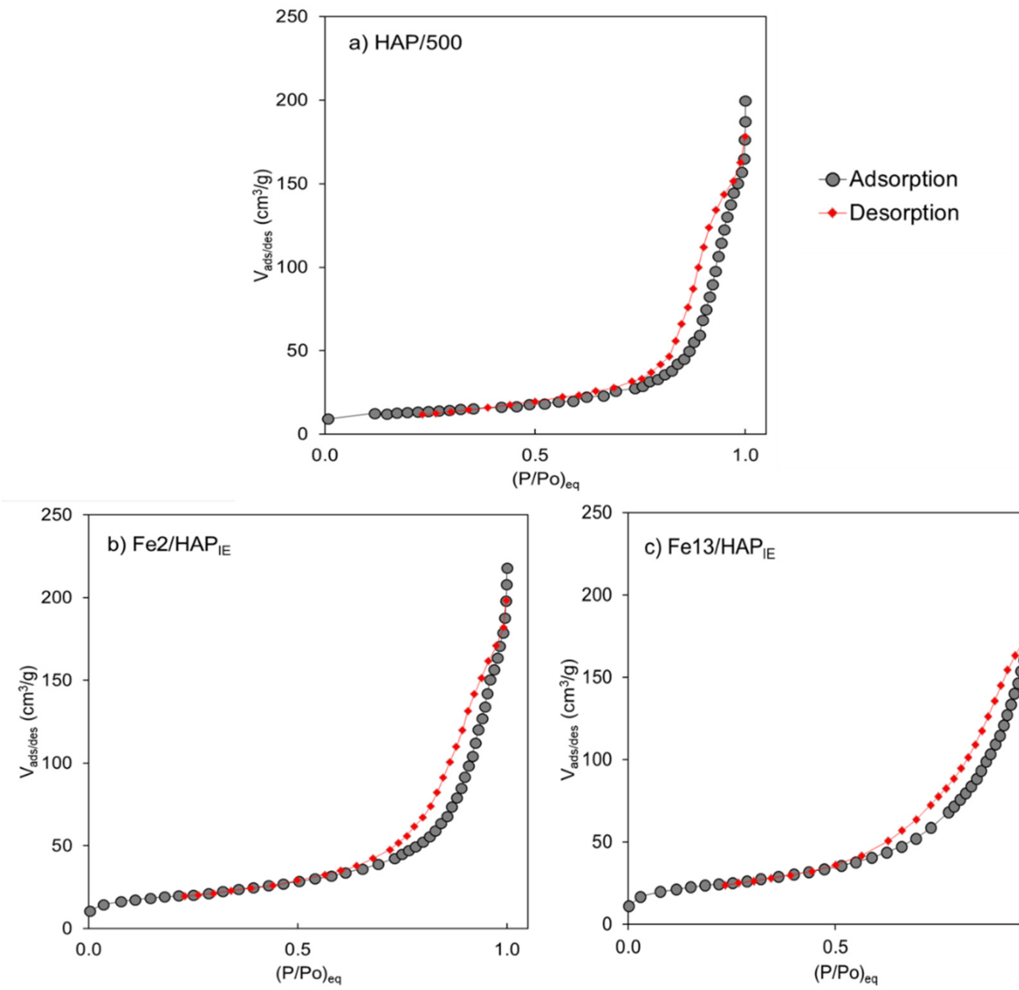

Figure S1 N_2 adsorption/desorption isotherms at -196°C of bare HAP calcined at 500°C (a) and of two Fe/HAP, presenting the lowest and the highest Fe-loading among Fe-loaded samples ($Fe2/HAP_{IE}$, b, and $Fe13/HAP_{IE}$, c, respectively).

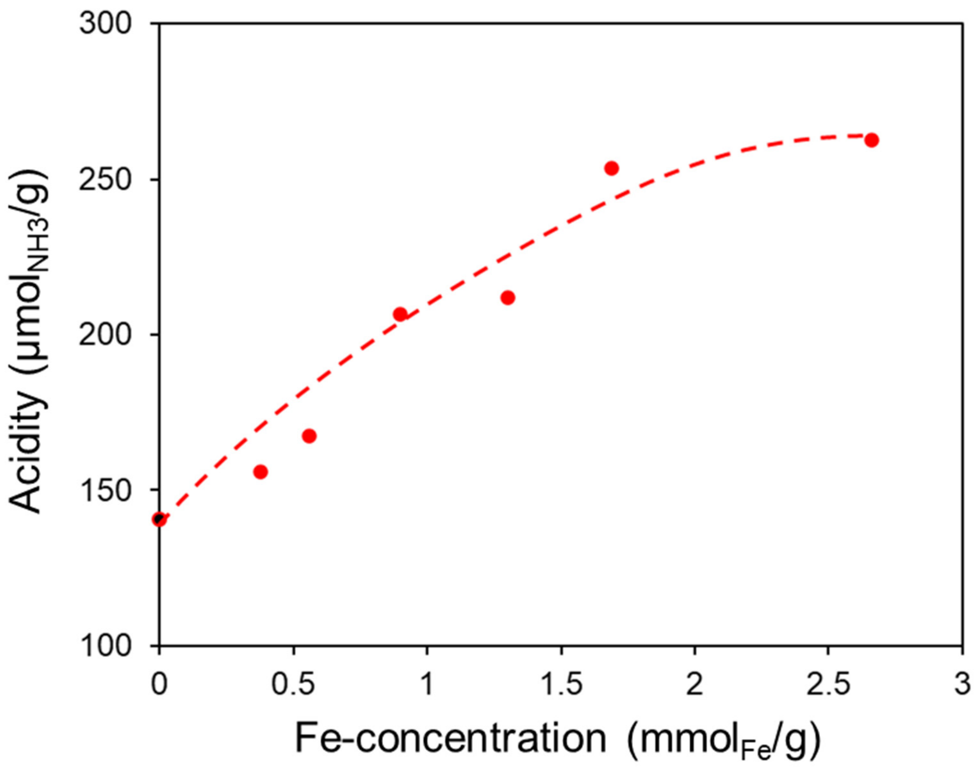

Figure S2 Acidity trend (in µmol$_{NH3}$/g) of Fe/HAP samples as a function of Fe-concentration (expressed in mmol$_{Fe}$/g) with indication of HAP acidity (black marker).

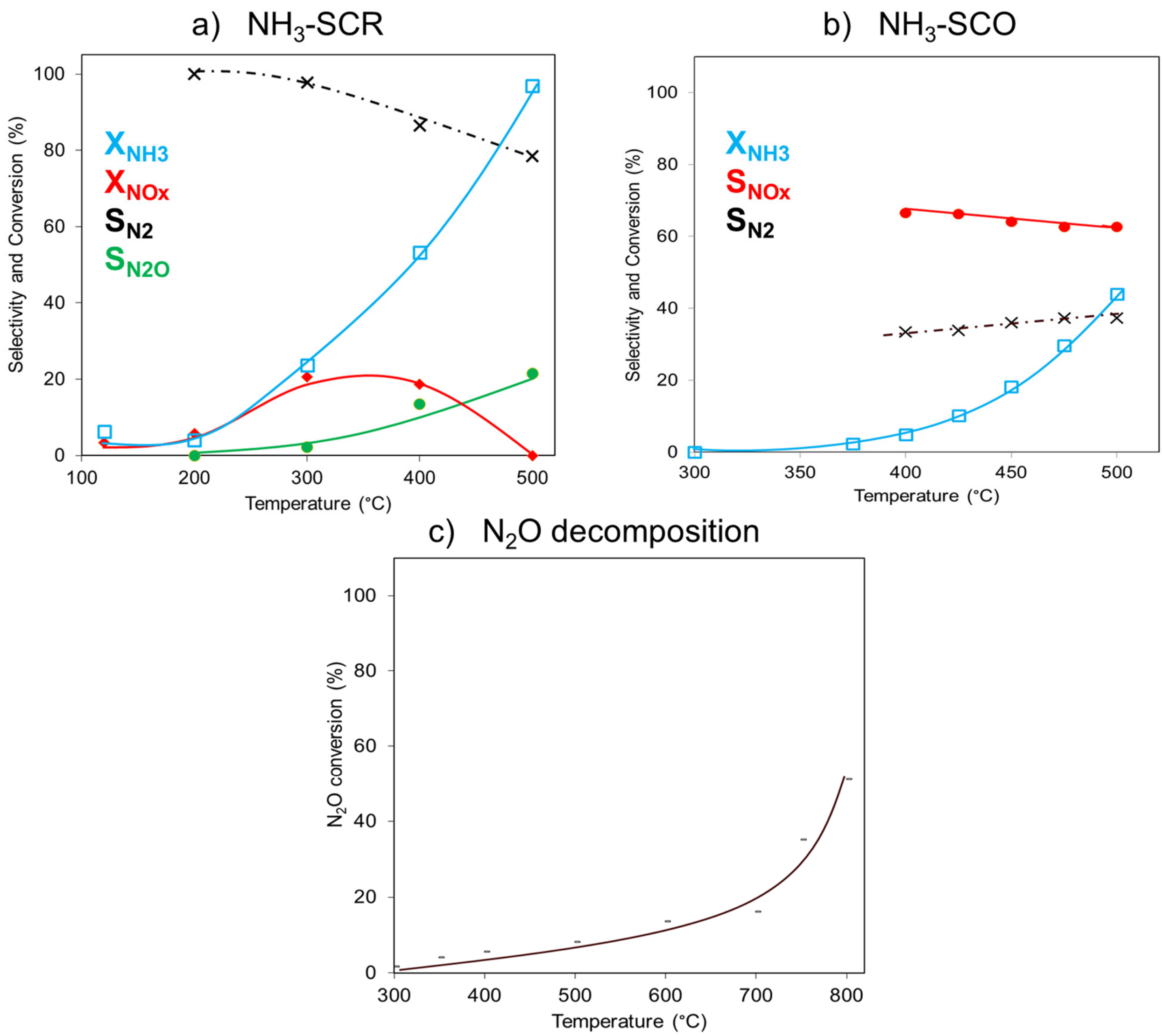

Figure S3 Catalytic activity results on bare HAP: a) NH_3-SCR: profiles of conversion of fed species (NH_3 and NOx) and formed species (N_2 and N_2O) as a function of temperature; b) NH_3-SCO: profiles of conversion of fed species (NH_3) and formed species (N_2 and NO_x) as a function of temperature; c) N_2O decomposition: profile of N_2O conversion as a function of temperature.

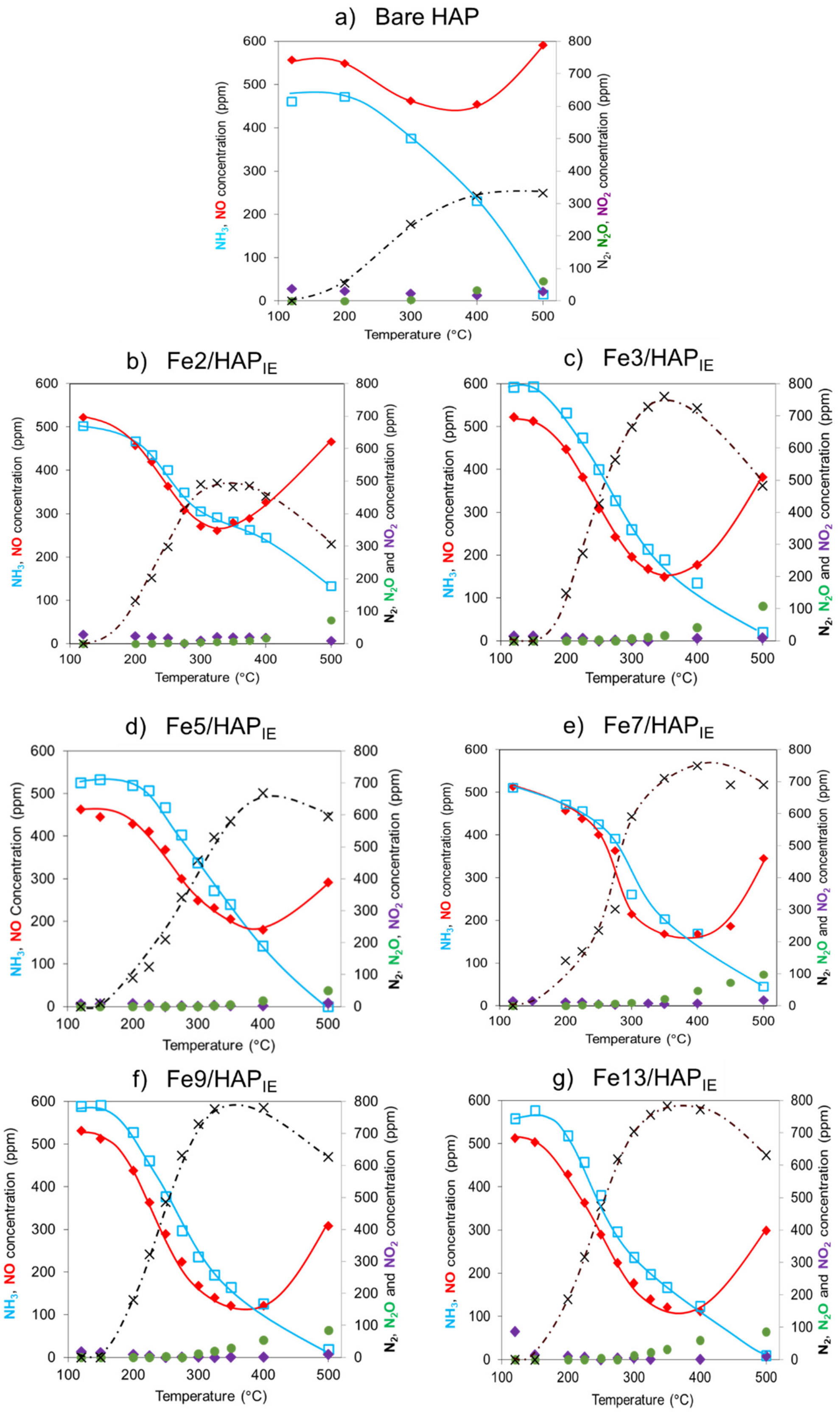

Figure S4 NH_3-SCR catalytic activity results on Fe/HAP samples: profiles of concentration of fed species (NH_3 and NO) and formed species (N_2 and N_2O, NO_2) as a function of temperature. Reaction conditions: [NH_3]=[NO]= 500 ppm, [O_2]=10,000 ppm; GHSV= 30,000 h^{-1}.

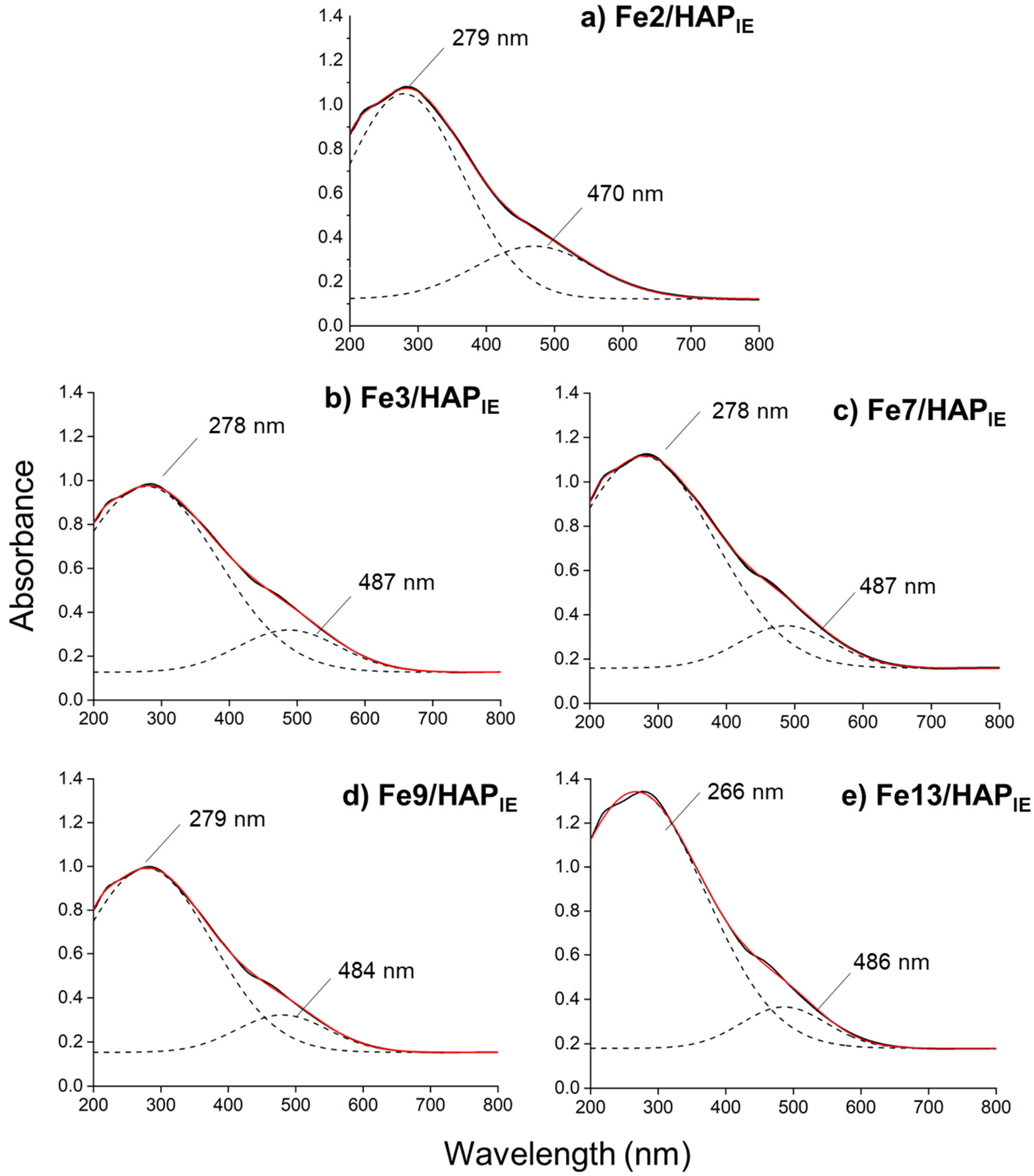

Figure S5 UV-vis DR spectra (black curves) of Fe/HAP samples (a-e): total calculated curves (red lines) and decomposed curves (dotted black lines) with the related peak centers are also reported.

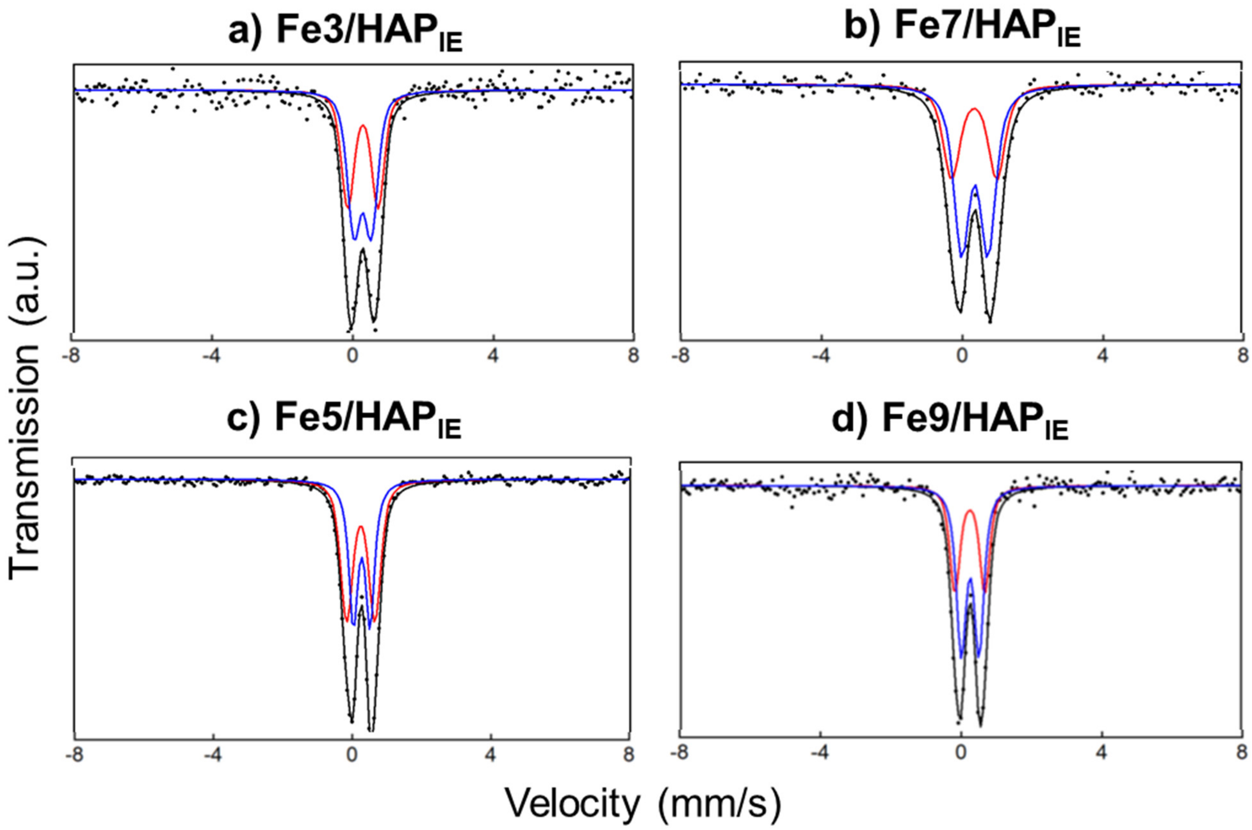

Figure S6 Mössbauer spectra of Fe/HAP samples (a-d) collected at room temperature.

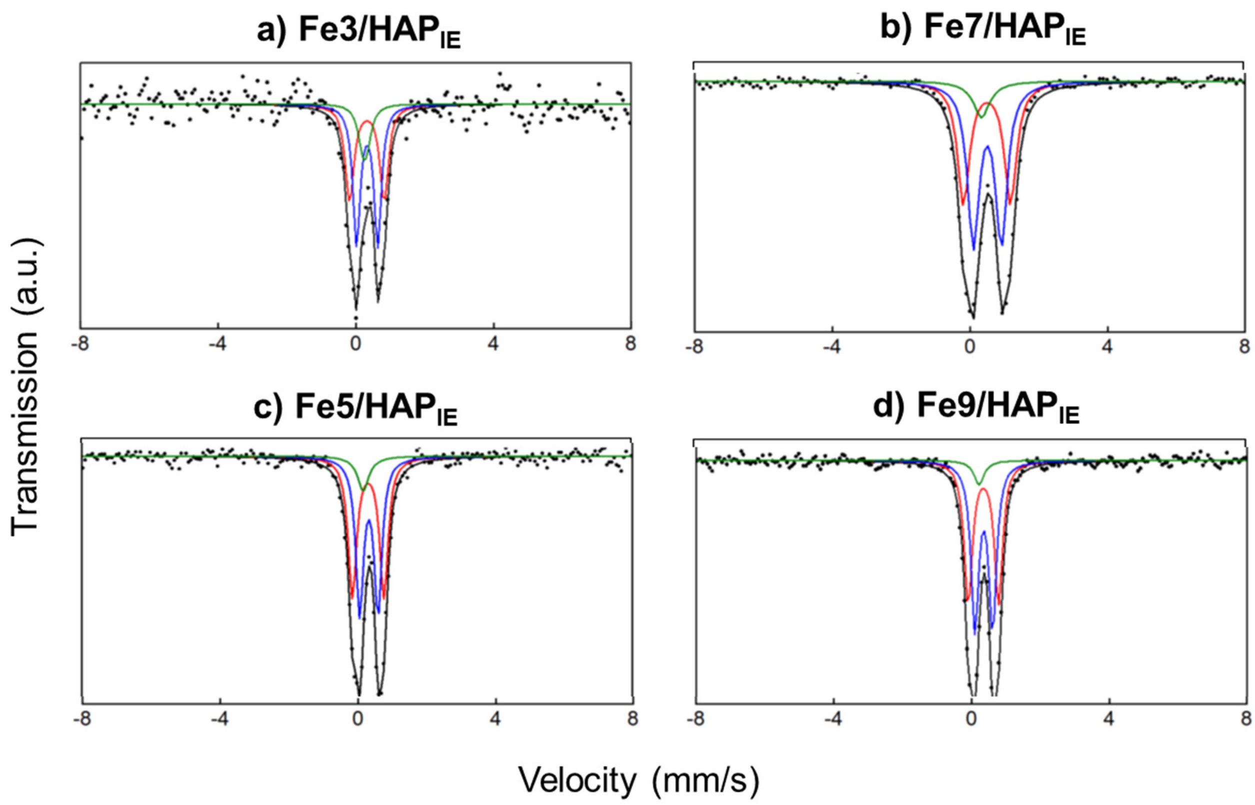

Figure S7 Mössbauer spectra of Fe/HAP samples (a-d) collected at -260°C.

Table S1. Symbols and calculations for computing catalytic parameters

F_{tot}	Gas flow rate ($NL \cdot h^{-1}$)
in	Feeding
out	Vented
X	Conversion (%)
S	Selectivity (%)

Catalytic Parameter	Unit	NH_3-SCR	NH_3-SCO	N_2O decomposition
θ_1 (contact time$_1$)	g·s/NL	$\frac{wcat}{Ftot} \cdot 3600$		
θ_2 (contact time$_2$)	g·s/mmol	$\frac{\theta_1 \cdot 22.414}{1000}$		
$[NO_x]$	ppm	[NO]+[NO_2]		-
$[N_2]$	ppm	$([NO_x]_{in} - [NO_x]_{out}) + ([NH_3]_{in} - [NH_3]_{out}) - 2[N_2O]_{out}$	$\frac{([NO_x]_{in} - [NO_x]_{out}) + ([NH_3]_{in} - [NH_3]_{out})}{2}$	-
X_{NOx}	%	$\frac{([NO_x]_{in} - [NO_x]_{out})}{[NO_x]_{in}} \cdot 100$	-	
S_{NOx}	%	-	S_{NO}+ S_{NO2}	-
X_{NH3}	%	$\frac{([NH_3]_{in} - [NH_3]_{out})}{[NH_3]_{in}} \cdot 100$	$\frac{([NH_3]_{in} - [NH_3]_{out})}{[NH_3]_{in}} \cdot 100$	-
S_{N2}	%	$\left(1 - \frac{(2 \cdot [N_2]_{out})}{([NO_x]_{in} - [NO_x]_{out}) + ([NH_3]_{in} - [NH_3]_{out})}\right) \cdot 100$	$\frac{2 \cdot ([N_2]_{out})}{([NH_3]_{in} - [NH_3]_{out})} \cdot 100$	-
X_{N2O}	%	-		$\frac{([N_2O]_{in} - [N_2O]_{out})}{[N_2O]_{in}} \cdot 100$
S_{N2O}	%	$\left(1 - \frac{([N_2O]_{out})}{([NO_x]_{in} - [NO_x]_{out}) + ([NH_3]_{in} - [NH_3]_{out})}\right) \cdot 100$	$\frac{2 \cdot ([N_2O]_{out})}{([NH_3]_{in} - [NH_3]_{out})} \cdot 100$	-

* where the $[species]_{in}$ are the by-pass concentrations and $[species]_{out}$ are the concentrations evaluated at steady-state conditions at each reaction temperature.

Table S2 Mössbauer parameters of all the Fe/HAP samples at room temperature.

Code	Parameters		
	Δ^a (mm/s)	δ^b (mm/s)	%^{c}
$Fe2/HAP_{IE}$	1.3 ± 0.3	0.37 ± 0.02	48 ± 28
	0.7 ± 0.1	0.40 ± 0.03	52 ± 28
$Fe3/HAP_{IE}$	1.27 ± 0.07	0.39 ± 0.01	36 ± 6
	0.76 ± 0.06	0.40 ± 0.01	62 ± 6
$Fe5/HAP_{IE}$	1.2 ± 0.2	0.37 ± 0.01	55 ± 16
	0.72 ± 0.04	0.41 ± 0.02	45 ± 16
$Fe7/HAP_{IE}$	1.3 ± 0.2	0.38 ± 0.03	38 ± 11
	0.76 ± 0.07	0.40 ± 0.02	66 ± 11
$Fe9/HAP_{IE}$	1.3 ± 0.1	0.38 ± 0.02	40 ± 8
	0.76 ± 0.04	0.39 ± 0.01	60 ± 8
$Fe13/HAP_{IE}$	1.27 ± 0.07	0.39 ± 0.01	38 ± 6
	0.76 ± 0.04	0.40 ± 0.01	62 ± 6

[a] quadrupole splitting; [b] isomer shift (all the isomer shifts are referred to α-Fe at 25°C); [c] normalized population of Fe^{3+} centres.

Table S3 Mössbauer parameters of all the Fe/HAP samples collected at -260 °C.

Code	Parameters					Fe species
	Δ^a (mm/s)	δ^b (mm/s)	$2\varepsilon^c$ (mm/s)	H^d (kOe)	%^{e}	
$Fe2/HAP_{IE}$	1.49 ± 0.08	0.54 ± 0.03	-	-	38 ± 6	Paramagnetic Fe^{3+} replacing Ca(2) ions
	0.80 ± 0.07	0.52 ± 0.02	-	-	47 ± 7	Paramagnetic Fe^{3+} replacing Ca(1) ions
	-	0.37 ± 0.08	0^f	450^f	15 ± 6	Fe_xO_y nanoclusters (2<size (nm)<4)
$Fe3/HAP_{IE}$	1.5 ± 0.1	0.47 ± 0.04	-	-	40 ± 10	Paramagnetic Fe^{3+} replacing Ca(2) ions
	0.92 ± 0.08	0.48 ± 0.02	-	-	46 ± 9	Paramagnetic Fe^{3+} replacing Ca(1) ions
	-	0.37^f	0^f	450^f	14 ± 5	Fe_xO_y nanoclusters (2<size (nm)<4)
$Fe5/HAP_{IE}$	1.36 ± 0.04	0.48 ± 0.01	-	-	46 ± 4	Paramagnetic Fe^{3+} replacing Ca(2) ions
	0.80 ± 0.04	0.51 ± 0.01	-	-	46 ± 5	Paramagnetic Fe^{3+} replacing Ca(1) ions
	-	0.27 ± 0.09	0^f	450^f	8 ± 3	Fe_xO_y nanoclusters (2<size (nm)<4)
$Fe7/HAP_{IE}$	1.37 ± 0.03	0.50 ± 0.01	-	-	40 ± 3	Paramagnetic Fe^{3+} replacing Ca(2) ions
	0.81 ± 0.03	0.51 ± 0.01	-	-	51 ± 3	Paramagnetic Fe^{3+} replacing Ca(1) ions
	-	0.34 ± 0.05	0^f	450^f	9 ± 2	Fe_xO_y nanoclusters (2<size (nm)<4)
$Fe9/HAP_{IE}$	1.31 ± 0.03	0.49 ± 0.01	-	-	46 ± 3	Paramagnetic Fe^{3+} replacing Ca(2) ions
	0.77 ± 0.03	0.50 ± 0.01	-	-	49 ± 3	Paramagnetic Fe^{3+} replacing Ca(1) ions
	-	0.30 ± 0.09	0^f	450^f	5 ± 2	Fe_xO_y nanoclusters (2<size (nm)<4)
$Fe13/HAP_{IE}$	1.28 ± 0.02	0.48 ± 0.01	-	-	42 ± 2	Paramagnetic Fe^{3+} replacing Ca(2) ions
	0.76 ± 0.02	0.50 ± 0.01	-	-	50 ± 2	Paramagnetic Fe^{3+} replacing Ca(1) ions
	-	0.38 ± 0.08	0^f	450^f	8 ± 2	Fe_xO_y nanoclusters (2<size (nm)<4)

[a] quadrupole splitting; [b] isomer shift (all the isomer shifts are referred to α-Fe at 25°C); [c] quadrupole shift; [d] hyperfine magnetic field; [e] normalized population of Fe^{3+} centres; [f] held parameters fixed in fitting.